Science of the Total Environment 609 (2017) 742–754

Contents lists available at ScienceDirect

Science of the Total Environment

journal homepage: www.elsevier.com/locate/scitotenv

Temporal trends of surface urban heat islands and associated determinants in major Chinese cities

Rui Yao [a], Lunche Wang [a,*], Xin Huang [b,c,**], Zigeng Niu [a], Fongfu Liu [a], Qing Wang [b]

[a] Laboratory of Critical Zone Evolution, School of Earth Sciences, China University of Geosciences, Wuhan 430074, China
[b] School of Remote Sensing and Information Engineering, Wuhan University, Wuhan 430079, China
[c] State Key Laboratory of Information Engineering in Surveying, Mapping and Remote Sensing, Wuhan University, Wuhan 430079, China

HIGHLIGHTS

- It is first time to study the temporal trends of SUHI at national scale.
- The surface urban heat island is intensifying in China.
- SUHII in SUA and UA was correlated with LST and urbanization, respectively.

GRAPHICAL ABSTRACT

Temporal trends of surface urban heat island intensity in China during 2001–2015. SUA: stable urban area. UA: urbanized area.

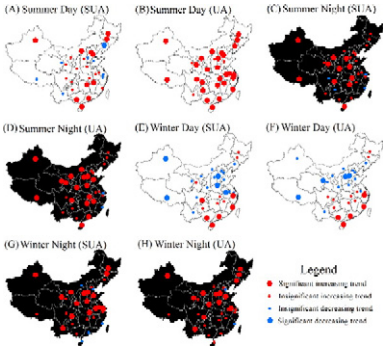

ARTICLE INFO

Article history:
Received 28 May 2017
Received in revised form 13 July 2017
Accepted 24 July 2017
Available online 28 July 2017

Editor: D. Barcelo

Keywords:
Surface urban heat island
Urbanization
Temporal trend
China

ABSTRACT

There are many studies focusing on spatial variations of surface urban heat islands (SUHIs) in literature. In this study, MODIS land surface temperature (LST) data and China's Land Use/Cover Datasets (CLUDs) were used to examine the temporal trends of SUHIs in 31 major Chinese cities during 2001–2015 using three indicators: SUHI intensity (SUHII), area of the SUHI ($Area_{SUHI}$) and percentage of area with increasing SUHII (PAISUHII). Correlation analyses between SUHII and background (rural) LST (extracted from MODIS LST), vegetation coverage (reflected by MODIS EVI data) and anthropogenic heat release (reflected by nighttime light data) were performed from temporal rather than spatial perspectives. Our findings showed that the SUHII and $Area_{SUHI}$ in urbanized areas increased significantly in most cities in summer days, whereas they increased significantly in approximately half and more than half of the cities in summer and winter nights, respectively. In summer days, summer nights and winter nights, the PAISUHII was approximately 80% and over 50% in union areas and the 20 km buffer, respectively. Correlation analyses indicated that the SUHII in stable urban areas was negatively correlated with the background LST in summer and winter days for most cities, especially in northern China. A reduction in vegetation contributed to the increasing SUHII in urbanized areas in summer days and nights. The increasing anthropogenic heat release was an important factor for increases in the SUHII in urbanized areas.

* Corresponding author.
** Co-corresponding author.
E-mail addresses: wang@cug.edu.cn (L. Wang), xhuang@whu.edu.cn (X. Huang).

http://dx.doi.org/10.1016/j.scitotenv.2017.07.217
0048-9697/

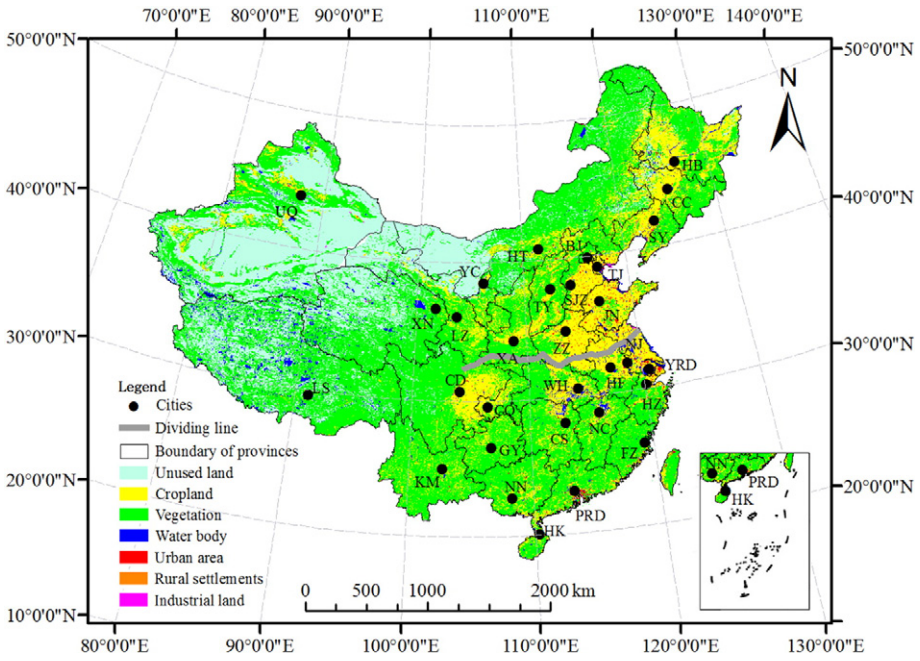

Fig. 1. The 31 selected Chinese cities in this study. The northern cities included Harbin (HB), Changchun (CC), Urumqi (UQ), Shenyang (SY), Hohhot (HT), Beijing (BJ), Tianjin (TJ), Yinchuan (YC), Shijiazhuang (SJZ), Taiyuan (TY), Jinan (JN), Xining (XN), Lanzhou (LZ), Zhengzhou (ZZ) and Xi'an (XA). The southern cities included Nanjing (NJ), Yangtze River Delta (YRD), Heifei (HF), Hangzhou (HZ), Wuhan (WH), Chengdu (CD), Chongqing (CQ), Nanchang (NC), Changsha (CS), Fuzhou (FZ), Guiyang (GY), Kunming (KM), Nanning (NN), Pearl River Delta (PRD) and Haikou (HK). Another city was Lhasa (LS). The background map was the China's Land Use/Cover Datasets (CLUDs) in 2010.

1. Introduction

Urbanization is accelerating all over the world. The urban population accounted for 30% and 54% of the total world population in 1951 and 2015, respectively, and this percentage is expected to reach 60% by 2030 (United Nations, 2014). Urbanization can cause a series of environmental issues that have profound impacts on human life, including the urban heat island (UHI) effect, which is defined as a higher temperature in urban areas than in rural areas (Peng et al., 2012; Zhou et al., 2015). This phenomenon can be attributed to: a) the increases in impervious surfaces can lead to the transformation from latent heat flux into sensible heat flux; b) the low albedo and high heat storages of urban roads and buildings; c) anthropogenic heat release. The UHI effect can influence human life by increasing the risk of exposure to health-threatening heat (Zhou et al., 2015) and energy consumption (Akbari et al., 2015), and it can also reduce water and air quality (Grimm et al., 2008; Zhou et al., 2014), change land surface phenology (Zhou et al., 2016c; Yao et al., 2017) and decrease net primary production (Chen et al., 2017; Imhoff et al., 2004). Therefore, both the magnitude and temporal trends of UHIs must be comprehensively studied.

UHIs include atmospheric UHIs monitored by weather stations and surface UHIs (SUHIs) estimated by remote sensing (Zhou et al., 2014). Although the atmospheric UHIs is more closely related to human health, Both types of UHIs are still highly related (Arnfield, 2003; Zhou et al., 2016b). The use of remote sensing to monitor SUHIs has attracted increasing attention around the world in recent decades because of its free access and broad spatial coverage. Studies have used Landsat TM/ETM + to study the time series of SUHI in a single city because of the high spatial resolution and long time series of products, and results have indicated that the SUHI has been intensifying or expanding in certain cities of China, including Beijing (Qiao et al., 2014), Shanghai (Zhao et al., 2016), Nanjing (Tu et al., 2016), Wuhan (Shen et al., 2016) and Lanzhou (Pan, 2015). Studies have also used MODIS land surface temperature (LST) data to study the spatiotemporal variations of SUHIs at regional or global scales (Clinton and Gong, 2013; Peng et al., 2012; Wang et al., 2015a; Zhou et al., 2016a; Zhou et al., 2014; Weng et al., 2014). The results of such studies have indicated that SUHIs were characterized by large spatial, diurnal and seasonal heterogeneity. For example, Peng et al. (2012) studied the SUHI intensity (SUHII, temperature difference between urban and rural areas) in 419 large cities worldwide for the period 2003–2008, and the results showed that the daytime SUHII was higher than the nighttime SUHII (1.5 ± 1.2 °C vs. 1.1 ± 0.5 °C, $p < 0.01$). Zhou et al. (2014) and Wang et al. (2015a) investigated the SUHII in 32 major Chinese cities for the period 2003–2011 and 67 large Chinese cities for the period 2003–2010, respectively, and results showed that the daytime SUHII was higher in summer and lower in winter while the nighttime SUHII was relatively stable across seasons. The daytime SUHII in southern cities was higher than that in northern cities, although the opposite occurred at night. Zhou et al.

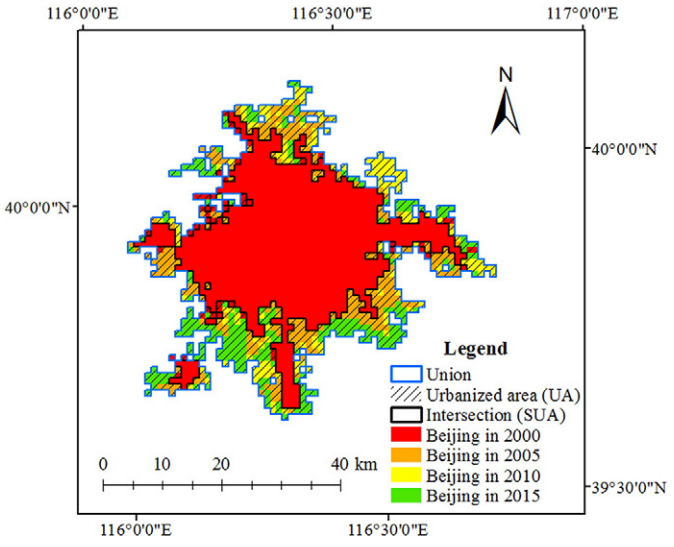

Fig. 2. The schematic diagram of old urban areas (SUAs) and urbanized areas (UAs), using BJ as an example. The background maps were CLUDs in 2000 (red), 2005 (orange), 2010 (yellow), 2015 (green).

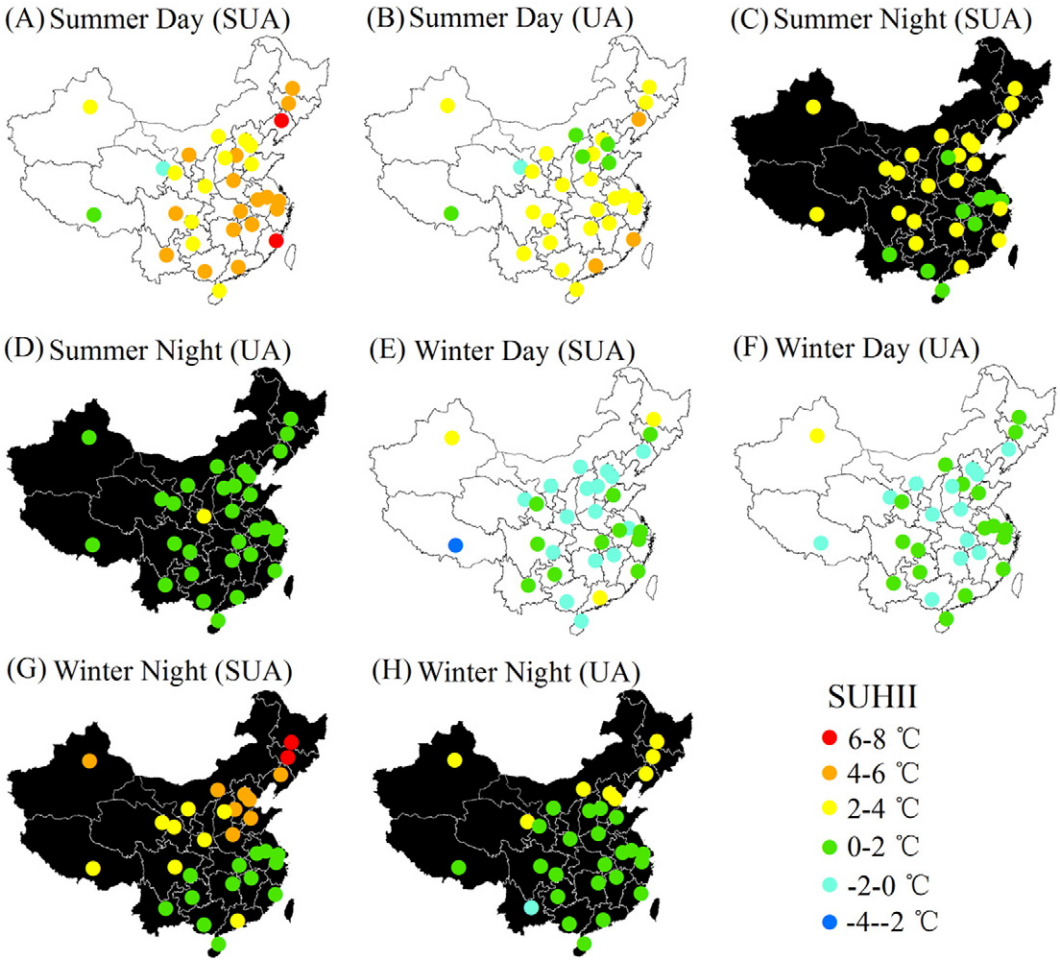

Fig. 3. Surface urban heat island intensity (SUHII) in each city averaged from 2001 to 2015.

(2015) showed that the LST decreased exponentially with increasing distances from urban areas and the UHI footprint for 31 major Chinese cities for the period 2003–2012 was 2.3 and 3.9 times larger than the area of the respective city during daytime and nighttime, respectively. However, in the context of rapid urbanization, few studies have performed a comprehensive analysis on the temporal trends of SUHI at regional or global scale. Only Zhou et al. (2016a) analyzed the temporal trends of SUHII according to the urban development intensity and both annual average daytime and nighttime SUHII increased significantly in only one-third of the cities in China for the period 2003–2012. Therefore, more studies about the temporal trends of SUHI and associated determinants across multiple cities should be conducted.

In addition, the relationships between SUHII and associated driving forces should be further studied. Previous studies have shown that albedo contributes greatly to the nighttime SUHII (Peng et al., 2012; Zhou et al., 2014) because urban roads and buildings have large heat storage, and the heat absorbed during the day is released slowly at night (Wang et al., 2016a). Vegetation can reduce the SUHII (Wang et al., 2016a), while anthropogenic heat release can increase SUHII in cities (Zhou et al., 2014; Peng et al., 2012). The relationships between SUHII and air temperature differed greatly in different areas (Du et al., 2016; Peng et al., 2012; Zhou et al., 2014). Although previous studies have conducted correlation analyses between SUHII and associated determinants across space (Du et al., 2016; Peng et al., 2012; Wang et al., 2015a; Zhou et al., 2016a; Zhou et al., 2016b; Zhou et al., 2014; Weng et al., 2008), the results of correlation analyses would differ if the analyses were conducted across different years. However, few studies have performed such studies at regional scales.

China has different climate zones that range from tropical in the south to subarctic in the north (Liang et al., 2016), and experiences a wide precipitation gradient that increases from the northwest to southeast (Zhou et al., 2014). As the largest developing country in the world, China has undergone continuous rapid urbanization in recent decades. The urban population in China has increased from 459 million in 2000 to 779 million in 2015 (United Nations, 2014), and the urban area has expanded from 4.85×10^4 km^2 in 1990 to 9.08×10^4 km^2 in 2010 (Kuang et al., 2016). Rapid urbanization has considerable impacts on the environment in China, and these impacts must be thoroughly investigated, particularly the temporal trends. To provide comprehensive and systematic research on the temporal trends of SUHI and fill the current research gaps, this study aimed to (1) examine the 15-year average SUHI in China; (2) investigate the temporal trends of SUHI for the period 2001–2015; and (3) analyze the relationships between SUHII and its driving forces.

2. Data and methods

2.1. Data

Two urban agglomerations and 29 municipalities or provincial capitals were selected in this study (Fig. 1). The two urban agglomerations were Pearl River Delta urban agglomeration (including Shenzhen, Dongguan, Guangzhou, Foshan, Zhongshan, Zhuhai, Xianggang and Jiangmen) and Yangtze River Delta urban agglomeration (including Shanghai, Suzhou, Changzhou and Wuxi). These areas have shown relatively faster urbanization in China and played an important role in China's economic development in recent decades (Du et al., 2016; Tao

Table 1
The mean surface urban heat island intensity (SUHII), mean Area of the surface urban heat island ($Area_{SUHI}$), mean area of the significant surface urban heat island ($Area_{SSUHI}$), trends of SUHII, trends of $Area_{SUHI}$, trends of $Area_{SSUHI}$ and percentage of area with increasing SUHII (PAISUHII) averaged for southern cities, northern cities and the whole study area during 2001–2015.

Region	SD	SN	WD	WN
Mean SUHII (°C)				
Southern cities (UA)	3.26	0.99	0.42	0.53
Northern cities (UA)	2.11	1.43	0.09	2.12
Whole study area (UA)	2.61	1.22	0.21	1.31
Southern cities (SUA)	4.79	1.89	0.40	1.42
Northern cities (SUA)	3.58	3.02	0.08	4.56
Whole study area (SUA)	4.09	2.48	0.16	2.96
Mean $Area_{SUHI}$ (km^2)				
Southern cities	1143.92	681.64	545.27	560.36
Northern cities	631.24	513.70	174.61	634.23
Whole study area	859.95	579.97	348.43	579.39
Mean $Area_{SSUHI}$ (km^2)				
Southern cities	979.37	268.7	251.61	226.96
Northern cities	459.63	299.91	82.56	452.37
Whole study area	696.83	276.39	161.70	329.41
Trends of SUHII (°C/year)				
Southern cities (UA)	0.180**	0.032**	0.046**	0.030*
Northern cities (UA)	0.132*	0.063**	−0.057**	0.073**
Whole study area (UA)	0.156**	0.052**	−0.010	0.051**
Southern cities (SUA)	0.039**	0.022**	0.073**	0.041*
Northern cities (SUA)	0.043*	0.043**	−0.074**	0.078**
Whole study area (SUA)	0.039**	0.038**	−0.004	0.059**
Trends of $Area_{SUHI}$ (km^2/year)				
Southern cities	24.72**	13.95**	15.73**	12.08*
Northern cities	17.63**	11.37**	−6.40	9.11**
Whole study area	20.54**	12.36**	4.49	10.29**
Trends of $Area_{SSUHI}$ (km^2/year)				
Southern cities	35.12**	8.25**	16.17**	7.09*
Northern cities	19.90**	9.10**	−1.53	10.51**
Whole study area	26.66**	8.49**	7.08**	8.54**
PAISUHII				
Southern cities (Union)	81.4%	73.4%	68.0%	73.4%
Northern cities (Union)	75.9%	85.9%	22.6%	84.5%
Whole study area (Union)	78.1%	80.2%	43.8%	79.2%
Southern cities (20 km buffer)	69.1%	54.5%	52.4%	62.8%
Northern cities (20 km buffer)	64.6%	60.4%	39.1%	52.3%
Whole study area (20 km buffer)	67.6%	58.2%	46.1%	56.0%

SD: summer day, SN: summer night, WD: winter day, WN: winter night.
* Significance level $p < 0.05$.
** Significance level $p < 0.01$.

et al., 2017; Zhang and Weng, 2016; Weng, 2002). The Qinling Mountain-Huaihe River Line was used to divide the study area into southern and northern parts (Wang et al., 2015a), with 15 southern cities (or urban agglomeration, hereafter), 15 northern cities and a plateau city (Lhasa).

The land cover data used in this study was China's Land Use/Cover Datasets (CLUDs) produced using Landsat TM/ETM + and HJ-1A/1B imagery. The original data (25 categories) were updated every five year from 1990 to 2015. The accuracy of all 25 categories of CLUDs was higher than 90% (Liu et al., 2014; Liu et al., 2010). Additional information about the CLUDs can be found in Kuang et al. (2016), Liu et al. (2010) and Liu et al. (2014).

The MOD11A2 product includes 8-day composite data at 1000 m spatial resolution, and it is an average of the MODIS daily LST product. These data were used to obtain the LST from 2001 to 2015 (Song et al., 2016; Zhou et al., 2014). The MODIS LST provides ideal data for studying the SUHI and has been used to analyze the spatial-temporal variations of SUHI at regional and global scales because of its wide coverage, high temporal resolution and high precision (Clinton and Gong, 2013; Du et al., 2016; Peng et al., 2012; Wang et al., 2015a; Zhou et al., 2014; Zhou et al., 2015). In addition, MOD13A2 enhanced vegetation index (EVI) data (16-day composite, 1000 m spatial resolution) was used to extract the vegetation information for the period 2001–2015. Finally, annual stable nighttime light (NL) data with a spatial resolution of 30″ were used as a surrogate for anthropogenic heat release from 2001 to 2013 (Peng et al., 2012; Zhou et al., 2014).

2.2. Methods

The CLUDs were first resampled to 1000 m spatial resolution to maintain consistency with MODIS data, and they were combined into four broad types (urban, rural settlements, water body and other land). Because of the cities' rapid expansion, their size and spatial extent differed in different years. Therefore, the urban areas must be divided before performing inter-annual analyses. The intersection of the urban areas in four land cover maps (for the years 2000, 2005, 2010 and 2015) was determined and defined as a stable urban area (SUA). That is to say, the SUA has always been urban area and did not experience land cover changes from 2001 to 2015. The SUA was then subtracted from the union of urban areas in the four land cover maps, and the resulting area was defined as an urbanized area (UA). That is to say, the UA has experienced land cover changes (mainly from other land cover types to urban areas) during 2001–2015. Next, we generated a 20 km buffer and a 20–25 km buffer based on the union areas, excluding the urban, industrial land and rural settlement pixels from the 20–25 km buffer, and defined this area as rural area (Zhou et al., 2016c). These approaches for dividing urban areas across years had two main advantages. First, these approaches facilitated a comparison of the LST in stationary areas (SUAs, UAs, union areas, 20 km buffer and rural areas) across different years. Second, compared with previous studies that used the dynamic but discontinuous urban extent from land cover maps (Zhou et al., 2016a; Zhou et al., 2014), our method divided urban areas into two stationary areas (SUAs and UAs) because this approach can eliminate errors introduced by rapid urbanization. The schematic diagram is shown in Fig. 2.

In this study, the temporal trends of SUHI were evaluated from three perspectives:

(1) SUHII. The LST differences between SUAs or UAs and rural areas were used to represent the SUHII (Peng et al., 2012; Zhou et al., 2014; Zhou et al., 2015), and the equations are described as follows:

$$\Delta T_{SUA} = T_{SUA} - T_{rural} \quad (1)$$

$$\Delta T_{UA} = T_{UA} - T_{rural} \quad (2)$$

where T_{SUA}, T_{UA} and T_{rural} are the LSTs in the SUA, UA and rural areas, respectively. Therefore, ΔT_{SUA} and ΔT_{UA} represent the SUHIIs in SUAs and UAs, respectively. In addition, water bodies and mountains were excluded based on previous studies (Imhoff et al., 2010; Zhou et al., 2015).

(2) Area of the SUHI ($Area_{SUHI}$). In each city, the number of pixels meeting the following requirements was defined as SUHI: 1) classified as built-up area (urban, rural settlements and industrial land, using CLUD in 2015); 2) in the union area and 20 km buffer; and 3) LSTs > 1 °C higher than the mean LST of the rural areas. The 1 °C was higher than the accuracy of MODIS LST data in most cases (Wan, 2008). The pixels with LSTs > 2 °C higher than the mean LST of the rural areas that met requirements 1) and 2) were defined as the area of significant SUHI ($Area_{SSUHI}$; Tran et al., 2006; Ward et al., 2016; Zhang and Wang, 2008). The $Area_{SUHI}$ was calculated as the number of pixel defined as SUHI multiplies the area of a MODIS LST pixel (1 km^2).

(3) Percentage of area with increasing SUHII (PAISUHII). We first calculated the SUHII using the same method in Eqs. (1) and (2) for each pixel and then calculated the linear changing rates of SUHII for each pixel from 2001 to 2015. Finally, we calculated the percentage of pixels with linear changing rates higher than zero in union areas and the 20 km buffer for each city. We

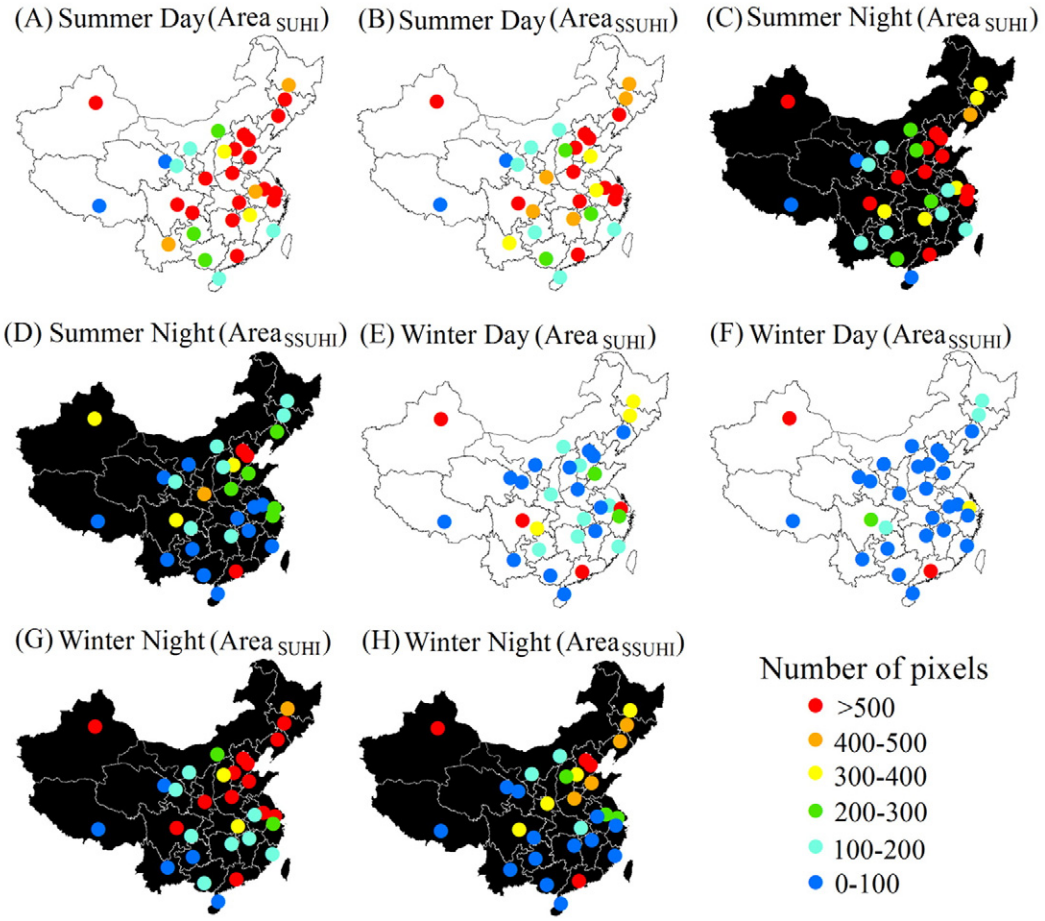

Fig. 4. Area of the surface urban heat island ($Area_{SUHI}$) and area of the significant surface urban heat island ($Area_{SSUHI}$) in each city averaged from 2001 to 2015.

hypothesized that the PAISUHII was equal to the percentage of pixels with increasing SUHII. If the PAISUHII was 90%, it suggested that 90% of the area experienced increasing SUHII from 2001 to 2015.

The MODIS LSTs from Terra satellite recorded at approximately 10:30 and 22:30 were used to represent the daytime and nighttime LST, respectively. The MOD11A2 data were averaged into summer (from June to August) and winter (from December to February) at corresponding date (ignoring no data pixels). Linear regression analyses were used to examine the temporal trends of SUHII, $Area_{SUHI}$ and $Area_{SSUHI}$. Significance tests ($p = 0.05$) were performed in SPSS 22.0 to examine whether significant differences in SUHI occurred across different seasons and regions.

The annual composite NL data during 2001–2013 were used as a proxy for the anthropogenic heat release according to previous studies (Peng et al., 2012; Zhou et al., 2014). However, inter-calibration, intra-annual composition and inter-annual corrections were required before using the NL data because of lacking of onboard calibration as well as sensor degradation and differences in radiometric performance (Huang et al., 2016; Liu et al., 2012). We used the same calibration method as Liu et al. (2012). Taiwan was used as a reference area because of its relatively stable nighttime light data values and economic development (Liu et al., 2012). Satellite F18 in the year 2010 was used as a reference for the inter-calibration because it has the highest cumulative data value (Elvidge et al., 2009; Liu et al., 2012). Inter-calibration equations can be found in Table S1.

To perform the correlation analysis, we calculated the ΔEVI using Eqs. (3) and (4), and calculated the ΔNL using Eqs. (5) and (6):

$$\Delta EVI_{SUA} = EVI_{SUA} - EVI_{rural} \quad (3)$$

$$\Delta EVI_{UA} = EVI_{UA} - EVI_{rural} \quad (4)$$

$$\Delta NL_{SUA} = NL_{SUA} - NL_{rural} \quad (5)$$

$$\Delta NL_{UA} = NL_{UA} - NL_{rural} \quad (6)$$

where EVI_{SUA}, EVI_{UA} and EVI_{rural} are EVI in SUA, UA and rural areas, respectively; NL_{SUA}, NL_{UA} and NL_{rural} are the NL in SUA, UA and rural areas, respectively.

T_{rural} was used to represent the background LST, and the inter-annual variations of T_{rural} were used to represent the background climate variability. We did not use the air temperature from weather stations because most weather stations were built in urban areas (Wang et al., 2015b), thus, the air temperature may be affected by UHI. Pearson's correlation analyses were conducted in SPSS 22.0 to examine the relationships between SUHII (ΔT_{SUA} or ΔT_{UA}) and vegetation coverage (ΔEVI_{SUA} or ΔEVI_{UA}), anthropogenic heat release (ΔNL_{SUA} or ΔNL_{UA}) or background climate variability (T_{rural}). Thus, we analyzed the mean and temporal trends of SUHI and their relationships with driving forces in each city at four different time periods (summer daytime, summer nighttime, winter daytime and winter nighttime) in two different types of urban area (SUA and UA) during 2001–2015.

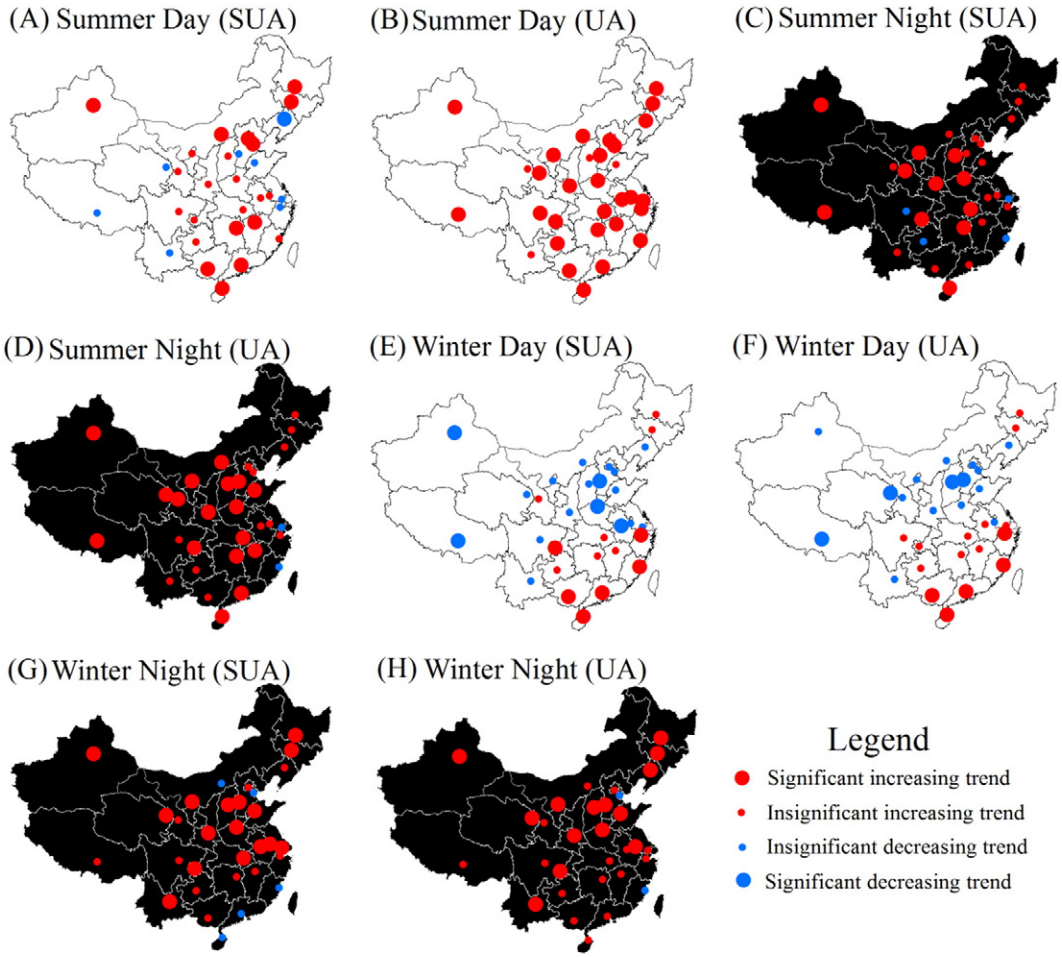

Fig. 5. Temporal trends of SUHII in each city from 2001 to 2015.

3. Results

3.1. Mean SUHII and $Area_{SUHI}$ in 31 major Chinese cities

The SUHII was evident in China (Fig. 3), the mean SUHII in SUA averaged for 31 cities was 4.09 °C in summer days, and the highest SUHII was observed in Shenyang (6.69 °C for SUA in summer days). Across all cities, the SUHII was significant higher in the SUAs than the UAs in summer days ($p < 0.01$), summer nights ($p < 0.01$) and winter nights ($p < 0.01$) (Table 1). However, significant differences were not observed in SUHII between the SUAs and UAs in winter days ($p > 0.05$). Spatially, the SUHII was higher in southern China than in northern China in summer days ($p < 0.05$) and winter days ($p > 0.05$) in the SUAs, but the opposite results were observed in summer nights ($p < 0.01$) and winter nights ($p < 0.01$) (Table 1). Similarly, the SUHII was higher in southern cities than in northern cities in summer days ($p < 0.01$) and winter days ($p > 0.05$) in the UAs, but the reverse results were found in summer nights ($p < 0.01$) and winter nights ($p < 0.01$) (Table 1).

The $Area_{SUHI}$ and $Area_{SSUHI}$ were evident in China (Fig. 4). The mean $Area_{SSUHI}$ averaged for 31 cities was 696.83 km^2 in summer days, and the largest $Area_{SSUHI}$ was observed in PRD (4671.73 km^2 in summer days). For all cities combined, the mean $Area_{SUHI}$ was 859.95 km^2, 579.97 km^2, 348.43 km^2 and 579.39 km^2 in summer days, summer nights, winter days and winter nights, respectively. In addition, the mean $Area_{SSUHI}$ was 696.83 km^2, 276.39 km^2, 161.7 km^2 and 329.41 km^2 in summer days, summer nights, winter days and winter nights, respectively. Spatially, both $Area_{SUHI}$ and $Area_{SSUHI}$ averages were significant larger for southern cities than for northern cities in summer days ($p < 0.01$) and winter days ($p < 0.01$, Table 1). The average $Area_{SSUHI}$ was larger for northern cities than southern cities in summer nights and winter nights ($p > 0.05$, Table 1). The average $Area_{SUHI}$ was higher for northern cities than southern cities in winter nights ($p > 0.05$), whereas the opposite was observed in summer nights ($p > 0.05$, Table 1).

3.2. PAISUHII, temporal trends of the SUHII, $Area_{SUHI}$ and $Area_{SSUHI}$ in major Chinese cities for the period 2001–2015

The SUHII was intensifying in China (Fig. 5). In summer days (including summer nights and winter nights), the SUHII increased in most cities for both SUAs and UAs (Fig. 5). Significant increasing trends of SUHII were observed in nearly half of the cities in the SUAs and UAs in summer nights and winter nights (Fig. 5). The SUHII increased significantly in 27 out of 31 cities for UAs in summer days. Across all cities, the SUHII increased significantly in summer days (0.039 °C/year, $p < 0.01$), summer nights (0.038 °C/year, $p < 0.01$) and winter nights (0.059 °C/year, $p < 0.01$) but decreased insignificantly in winter days (−0.004 °C/year, $p > 0.05$) in SUAs (Table 1). Concurrently, the SUHII increased significantly in summer days (0.156 °C/year, $p < 0.01$), summer nights (0.052 °C/year, $p < 0.01$) and winter nights (0.051 °C/year, $p < 0.01$) but decreased insignificantly in winter days (−0.01 °C/year, $p > 0.05$) in the UAs (Table 1). The highest increasing rate of SUHII was observed in Hefei (0.297 °C/year, in summer days in UA). Spatially, the SUHII in southern cities and northern cities showed opposite temporal trends in winter days. Across the 15 southern cities, the SUHII increased significantly at the rate of 0.073 °C/year ($p < 0.01$) and 0.046 °C/year ($p < 0.01$) in SUAs and UAs, respectively, in winter days (Table 1). However, across the 15 northern cities, the SUHII decreased significantly at the rate of

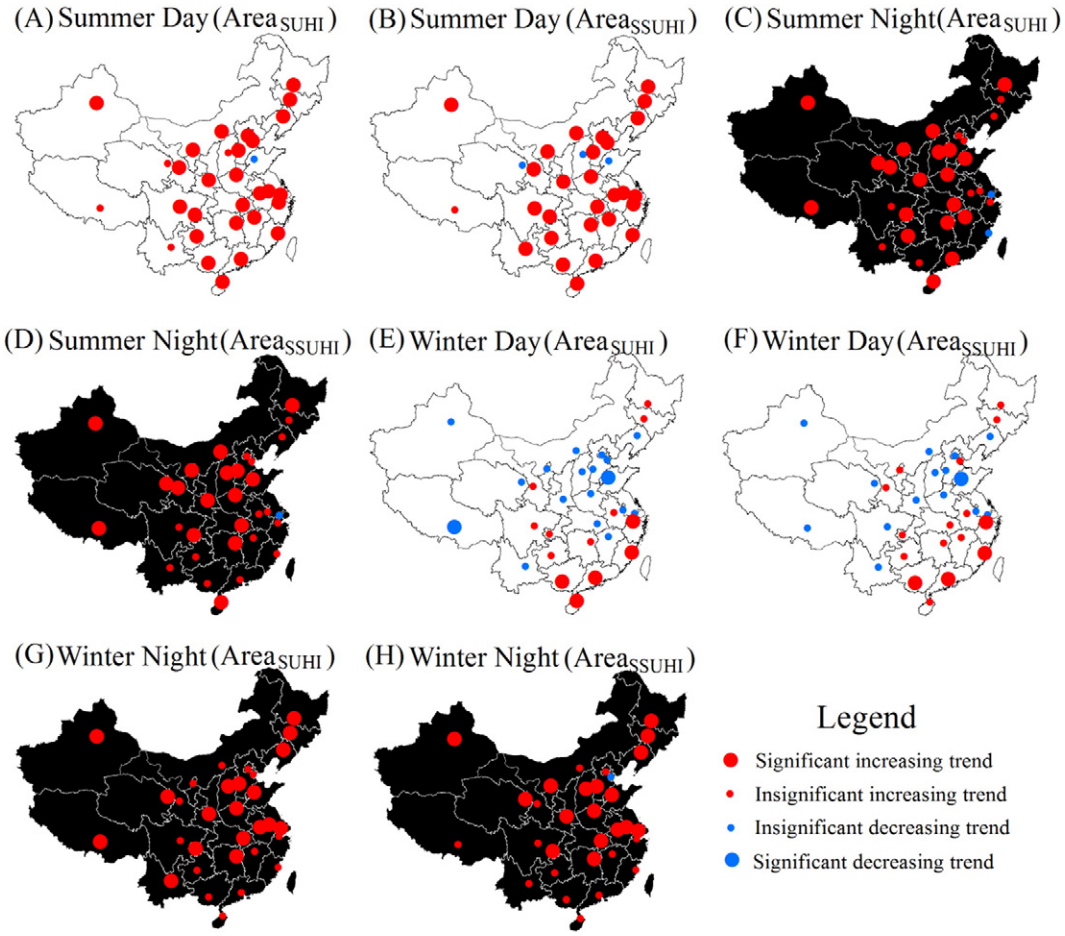

Fig. 6. Temporal trends of $Area_{SUHI}$ and $Area_{SSUHI}$ in each city from 2001 to 2015.

−0.074 °C/year ($p < 0.01$) and −0.057 °C/year ($p < 0.01$) in SUAs and UAs in winter days, respectively (Table 1). In summer nights and winter nights, the increasing rates of SUHII averaged for the northern cities were nearly twice as high as those of southern cities in both SUAs and UAs (Table 1).

The $Area_{SUHI}$ was accelerating in China (Fig. 6). The $Area_{SUHI}$ and $Area_{SSUHI}$ increased in most cities in summer days, summer nights and winter nights. Significant increasing trends in the $Area_{SUHI}$ and $Area_{SSUHI}$ were observed in over half of the cities in summer days, summer nights and winter nights (Fig. 6). For all cities, the $Area_{SUHI}$ increased significantly in summer days (20.54 km^2/year, $p < 0.01$), summer nights (12.36 km^2/year, $p < 0.01$) and winter nights (10.29 km^2/year, $p < 0.01$) but increased insignificantly in winter days (4.49 km^2/year, $p > 0.05$). Beijing witnessed the highest increasing rate of $Area_{SUHI}$ (82.2 km^2/year in summer days). In addition, the $Area_{SSUHI}$ increased significantly in summer days (26.66 km^2/year, $p < 0.01$), summer nights (8.49 km^2/year, $p < 0.01$), winter days (7.08 km^2/year, $p < 0.01$) and winter nights (8.54 km^2/year, $p < 0.01$). YRD witnessed the highest increasing rate of $Area_{SSUHI}$ (122.03 km^2/year in summer days). Spatially, the $Area_{SUHI}$ and $Area_{SSUHI}$ in summer days increased significantly in most (both southern and northern cities) cities (Fig. 6). However, the number of cities with significant increasing trends of $Area_{SUHI}$ and $Area_{SSUHI}$ was much greater in northern China than in southern China (11 vs. 7 for $Area_{SUHI}$ and 11 vs. 4 for $Area_{SSUHI}$) in summer nights. Similar results were observed in winter nights (10 vs. 7 for $Area_{SUHI}$ and 11 vs. 6 for $Area_{SSUHI}$). In addition, the $Area_{SUHI}$ and $Area_{SSUHI}$ in winter days increased in most cities in southern China but decreased in most cities in northern China (Fig. 6).

The SUHII increased in most study areas (Fig. 7). For all cities combined, the PAISUHII in union areas (see Methods and Fig. 2) was 78.1%, 80.2%, 43.8% and 79.2% in summer days, summer nights, winter days and winter nights, respectively. The highest PAISUHII was observed in Hohhot (100%, in summer days). The PAISUHII in 20 km buffer was 67.6%, 58.2%, 46.1% and 56.0% in summer days, summer nights, winter days and winter nights, respectively (Table 1). Spatially, the average PAISUHII for southern cities was similar to that for northern cities in summer days, summer nights and winter nights (Table 1). However, large differences in the PAISUHII were observed between southern cities and northern cities in winter days, and the average values in union areas and the 20 km buffer of southern and northern cities were 68.0% and 22.6%, respectively, and 52.4% and 39.1%, respectively.

3.3. Relationships between the SUHII and associated driving forces

The SUHII was negatively correlated with ΔEVI at most cities in summer, especially in the UAs (Fig. 8). Significant negative correlations between the SUHII and ΔEVI were found in 26 out of 31 cities in UAs in summer days, and nearly half of the cities (14 out of 31) had significant negative correlations between SUHII and ΔEVI in UAs. The decreasing ΔEVI may contribute to the increasing SUHII in both summer days and summer nights. In addition, the SUHII was negatively correlated with ΔEVI in most southern cities in winter, whereas it was significantly positive correlated with ΔEVI in several cities for winter days and winter nights.

In summer days and winter days, the SUHII in SUAs was negatively correlated with T_{rural} in most cities, especially in northern China (Fig. 9). In summer days, the SUHII was significantly negatively correlated with T_{rural} in over half (8 out of 15) of the northern cities in SUAs. In winter days, significant negative correlations between the SUHII and T_{rural} were found in 10 and 8 out of 15 northern cities in SUAs and UAs, respectively. These results indicated that the SUHII in SUAs was

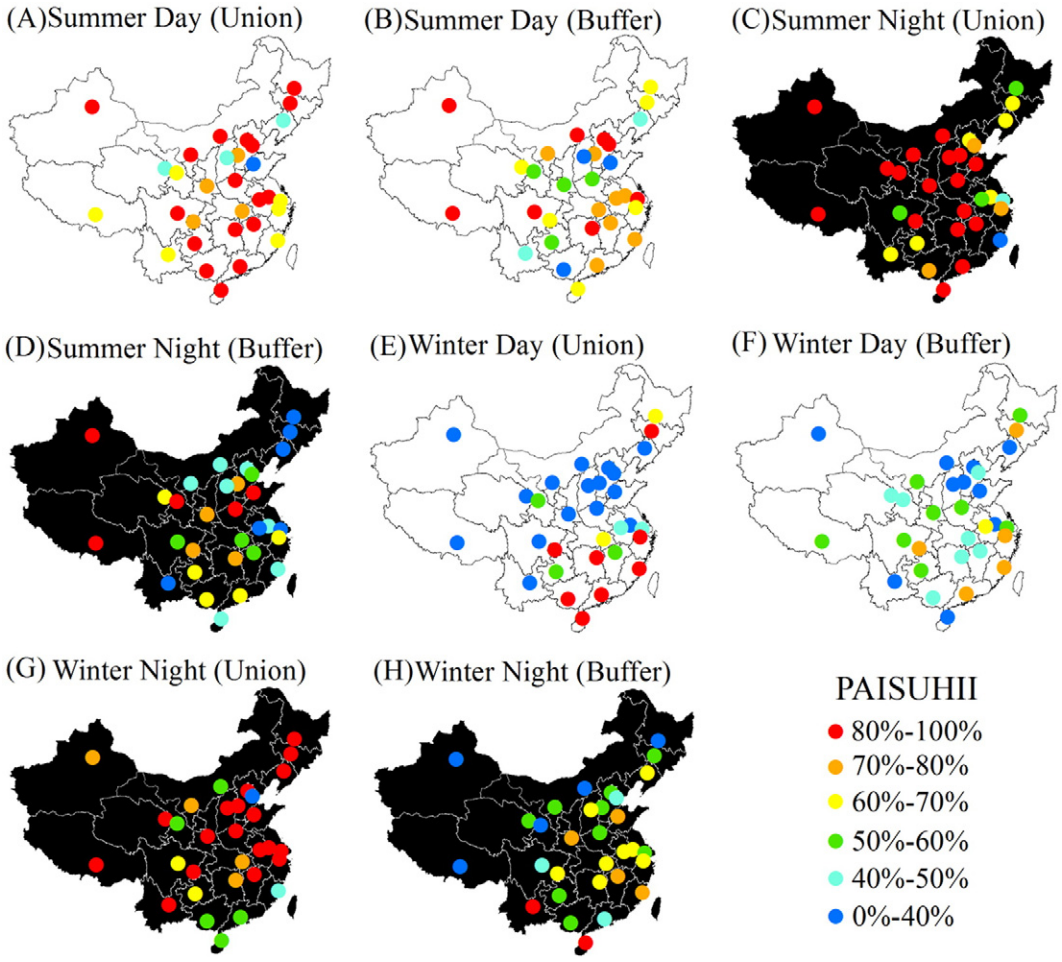

Fig. 7. Percentage of area with increasing SUHII (PAISUHII) in each city during 2001–2015.

affected by the inter-annual background climate variability in summer days and winter days, and these effects were more obvious in northern China than southern China.

The SUHII was positively correlated with △NL at most cities for UAs in summer days, summer nights and winter nights (Fig. 10). The number of cities with significant positive correlations between SUHII and △NL in UA was 21, 12 and 7 in summer days, summer nights and winter nights, respectively. The increasing △NL may contribute to the increases of SUHII in the UAs.

4. Discussion

4.1. Mean SUHII and Area$_{SUHI}$ in major Chinese cities

In this study, the SUHII was significantly higher in SUAs than UAs in summer days, summer nights and winter nights, which was likely due to the fact that the SUAs had higher anthropogenic heat release, lower vegetation coverage and albedo than the UAs. In addition, the SUHII was higher in southern cities than northern cities in summer days and winter days, although the opposite results were found in summer nights and winter nights. These results are consistent with previous studies (Wang et al., 2015a; Zhou et al., 2014). Northern cities generally have lower vegetation coverage in rural areas and higher △EVI than southern cities, which may lead to the lower daytime SUHII (Wang et al., 2015a; Zhou et al., 2014). Southern cities generally have higher soil moisture than northern cities because of the humid climate, which results in lower nighttime SUHII (Zhou et al., 2014). Finally, the 15-year averaged SUHII (Table 1) in this study was higher than that in Zhou et al. (2014) (1.93 °C in summer days; 0.23 °C in winter days; 1.02 °C in summer nights; 1.23 °C in winter nights), which studied the mean SUHII in 32 major cities in China during 2003–2011. The rural areas (20–25 km) in this study were much further from urban areas than the rural areas of Zhou et al. (2014). Previous studies have shown that the LST gradually decreased with increasing distance from urban areas (Han and Xu, 2013; Zhang et al., 2004) and included urban areas as well as suburbs in the footprint of the SUHII (Zhou et al., 2015). Yao et al. (2017) also showed that the SUHII increased significantly in 2 km buffer in Northeast China during 2001–2015. Therefore, for more accurate SUHII values, rural areas should be set at further distances from urban areas (Zhou et al., 2015). The reference rural area (20–25 km) was not extended farther for the purpose of minimizing the impacts of different background climate (Zhou et al., 2015). Based on the hypothesis that urban and rural have the same climate conditions, we calculated the SUHII by comparing the urban and rural LST differences. If the urban and rural areas have different climates (e.g. the urban area is raining but the rural area is sunny), the SUHII may be influenced by the climate conditions.

The seasonal, diurnal and spatial variations of mean Area$_{SUHI}$ and Area$_{SSUHI}$ were similar to that of the mean SUHII, with largest Area$_{SUHI}$ and Area$_{SSUHI}$ being observed in summer days, the smallest Area$_{SUHI}$ and Area$_{SSUHI}$ were observed in winter days. The southern cities had larger Area$_{SUHI}$ and Area$_{SSUHI}$ than the northern cities in summer and winter days, whereas the opposite results were observed in summer and winter nights.

4.2. Temporal trends of the SUHI in major Chinese cities for 2001–2015

The temporal trends of SUHI were systematically analyzed in 31 major cities in China for the period 2001–2015 using SUHII, Area$_{SUHI}$

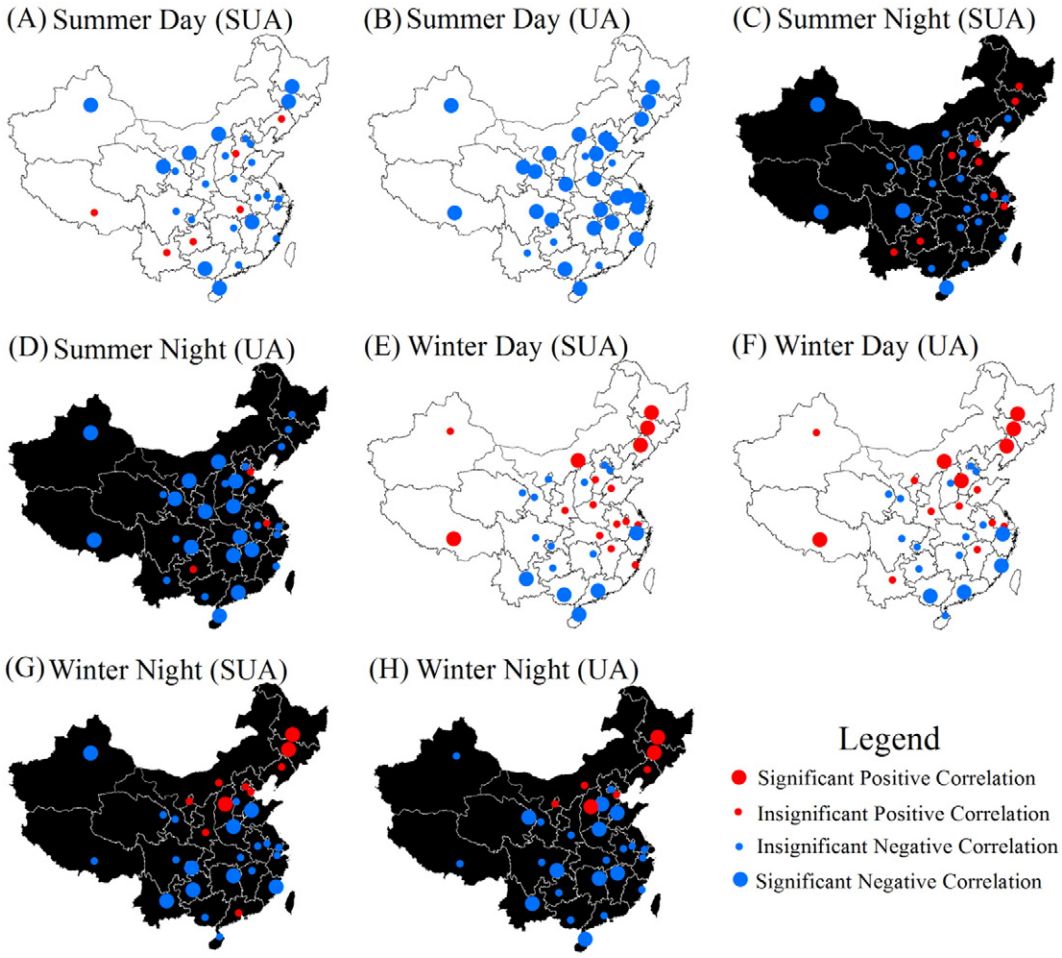

Fig. 8. Pearson's correlation analyses between SUHII and △EVI in each city during 2001–2015.

and PAISUHII. The SUHI in major Chinese cities experienced considerable changes over the study period. In summer days, summer nights and winter nights, the SUHII, $Area_{SUHI}$ and $Area_{SSUHI}$ in most cities increased over the study period, and increasing trends in SUHII were observed in approximately 80% of the union areas. These results may have been caused by three factors. Firstly, the decreasing vegetation coverage with rapid urbanization can lead to decreasing evapotranspiration, thereby strengthening the SUHII. Secondly, the impervious surfaces (roads and buildings) increase with urbanization, and can absorb heat from sunshine during the daytime and then release it slowly at night (Wang et al., 2016a). This leads to higher LSTs in urban areas than rural counterparts during both daytime and nighttime. Thirdly, the increases in anthropogenic heat release can transform into sensible heat flux and indirectly increase the LST (Zhou et al., 2014). In addition, there was about 20% of area with decreasing SUHII. This can be attributed to the policy of creating and preserving green areas provided by Chinese government (Zhou et al., 2016a). Zhou et al. (2016a) showed that the average annual daytime and nighttime SUHII increased significantly in only one-third of the 32 cities in China for the period 2003–2012. The temporal trends of daytime SUHI differed greatly by season in this study.

The SUHI underwent the greatest changes in summer days, although almost no significant increasing trends in SUHI were observed in winter days. The highest PAISUHII and increasing rates of SUHII, $Area_{SUHI}$ and $Area_{SSUHI}$ were all observed in summer days (Table 1, Figs. 5, 6 and 7). Two reasons may lead to above phenomena. Firstly, vegetation activity is considerably greater in summer than in winter and vegetation evapotranspiration occurs during the daytime. Therefore, the influences of decreasing vegetation coverage on SUHI were more evident in summer days. Secondly, the increasing impervious surfaces can absorb more heat during the daytime in summer than in winter because of the longer sunshine duration and larger direct solar radiation.

Spatially, opposite trends were observed in SUHI between northern China and southern China in winter days. The SUHII, $Area_{SUHI}$ and $Area_{SSUHI}$ increased at most cities in southern China but decreased at most cities in northern China, which may be explained by the vegetation activities. Certain southern cities were surrounded by evergreen forests and the EVI was still high in rural areas in winter, thus, the influence of decreasing vegetated areas on SUHI was still great in winter. The cities with highest EVI in winter (Chengdu, Fuzhou, Haikou, Kunming, Nanning, Pearl River Delta Urban Agglomeration and Hangzhou) included all cities with significant increasing SUHII in winter days (Fuzhou, Haikou, Nanning, Pearl River Delta Urban Agglomeration and Hangzhou). In addition, the increasingly serious air pollution in northern China can decrease the solar radiation and SUHII (Zhou et al., 2014).

In addition, the PAISUHII in union areas was higher in northern cities than in southern cities in summer nights and winter nights. The northern cities witnessed higher increasing trends in the SUHII, $Area_{SUHI}$ and $Area_{SSUHI}$ than southern cities in summer nights and winter nights (Table 1). These results can also be attributed to the higher soil moisture in southern cities than northern cities (Zhou et al., 2014). Higher soil moisture can lead to a slower cooling rate in rural areas and then limit the growth of SUHI during nighttime (Winguth and Kelp, 2013; Zhou et al., 2014).

Overall, the SUHI is intensifying and expanding in China during 2001–2015, and this trend may continue in next decades because of the urbanization. Problems related to human lives and environment may become more serious because of increases in severity of SUHI.

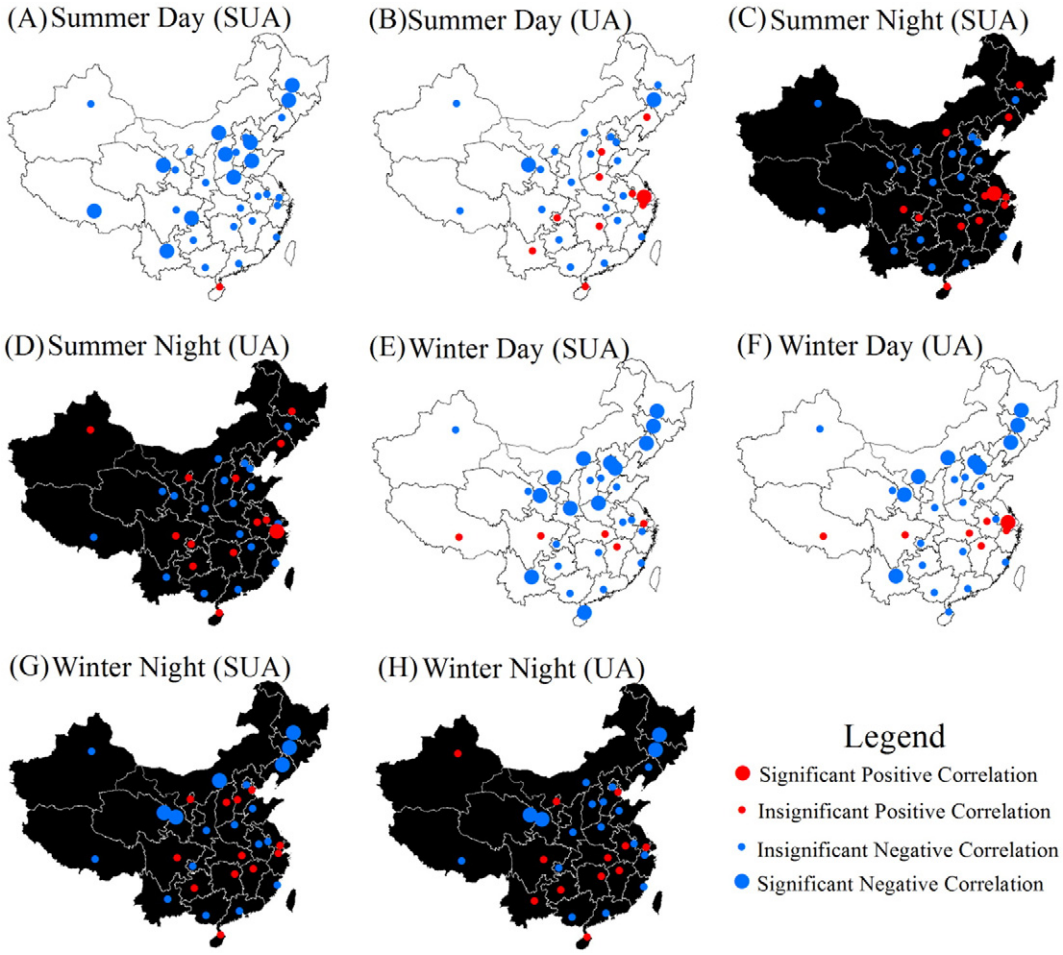

Fig. 9. Pearson's correlation analyses between SUHII and T_{rural} in each city during 2001–2015.

Therefore, the measures for mitigating UHI should be taken, such as increasing the vegetation coverage (Peng et al., 2012; Wang et al., 2016a; Maimaitiyiming et al., 2014; Qiao et al., 2013) and using cool pavement and roofs (Roman et al., 2016; Wang et al., 2016b). In addition, the increases in SUHII may have some potential benefits, for example, reducing the heating needs in cooler cities in winter.

Although a great number of studies analyzed the temporal trends of air UHI, very few studies have investigated the temporal trends of SUHI (Wang et al., 2015b). The significant increasing trend ($p < 0.05$) of air UHI was observed in intense urbanization area in China during 1951–2010, however, according to Wang et al. (2015b), the increasing rate of air UHII (0.0074 °C/year) was much lower than the increasing rate of SUHII in this study (Table 1). The different properties of air temperature and LST might lead to this phenomenon.

4.3. Relationships between the SUHII and associated driving forces

Previous studies have conducted correlation analyses between SUHII and associated driving forces in different cities (Du et al., 2016; Peng et al., 2012; Wang et al., 2015a; Zhou et al., 2016a; Zhou et al., 2016b; Zhou et al., 2014). In this study, correlation analyses were performed at each city over time, and certain interesting results were obtained.

The SUHII was negatively correlated with △EVI in summer days in most cities, especially in UAs (26 out of 31 cities with significant negative correlations). This finding suggests that vegetation could mitigate the SUHII in summer days, which is consistent with previous studies (Peng et al., 2012; Wang et al., 2015a; Zhou et al., 2014). Next, the SUHII was also negatively correlated with △EVI in most cities in summer nights, especially in UAs (14 out of 31 cities with significant negative correlations). This finding suggests that the vegetation coverage may also reduce the SUHII in summer nights, which is inconsistent with results of Peng et al. (2012), Zhou et al. (2014) and Zhou et al. (2016b), which performed correlation analyses across cities and the SUHII was invariant with △EVI at night. However, the results are similar to that of Quan et al. (2016), which conducted correlation analyses over time and NDVI was significantly negatively correlated with nighttime LST in urban areas in Beijing for the period 2000–2012. Doick et al. (2014) and Wang et al. (2016b) showed that vegetation can also reduce the nighttime UHII due to the fact that increasing vegetation cover can bring shading effects and reduce the amount of heat stored during the daytime and then reduce the nighttime SUHII (Quan et al., 2016; Tiangco et al., 2008). In addition, the SUHII was significantly negatively correlated with △EVI in several southern cities for winter days and winter nights. These results are inconsistent with Peng et al. (2012) and Zhou et al. (2014), which showed that the SUHII was not significantly correlated with △EVI in winter. In fact, certain cities in southern China are surrounded by evergreen forest, thus, with rapid urbanization, the EVI may also decrease rapidly and lead to increases in SUHII in winter. Finally, the SUHII was significantly positively correlated with △EVI in certain northern cities in winter days and winter nights, which may be resulted from the spurious EVI values (winter snow) (Piao, 2003; Zhou et al., 2014).

The correlation analyses showed that the SUHII in SUAs was negatively correlated with T_{rural} in most cities in summer days and winter days, especially in northern cities (Fig. 9). These results are inconsistent with Du et al. (2016), Zhou et al. (2014) and Zhou et al. (2016b), which performed correlation analyses between SUHII and air temperature

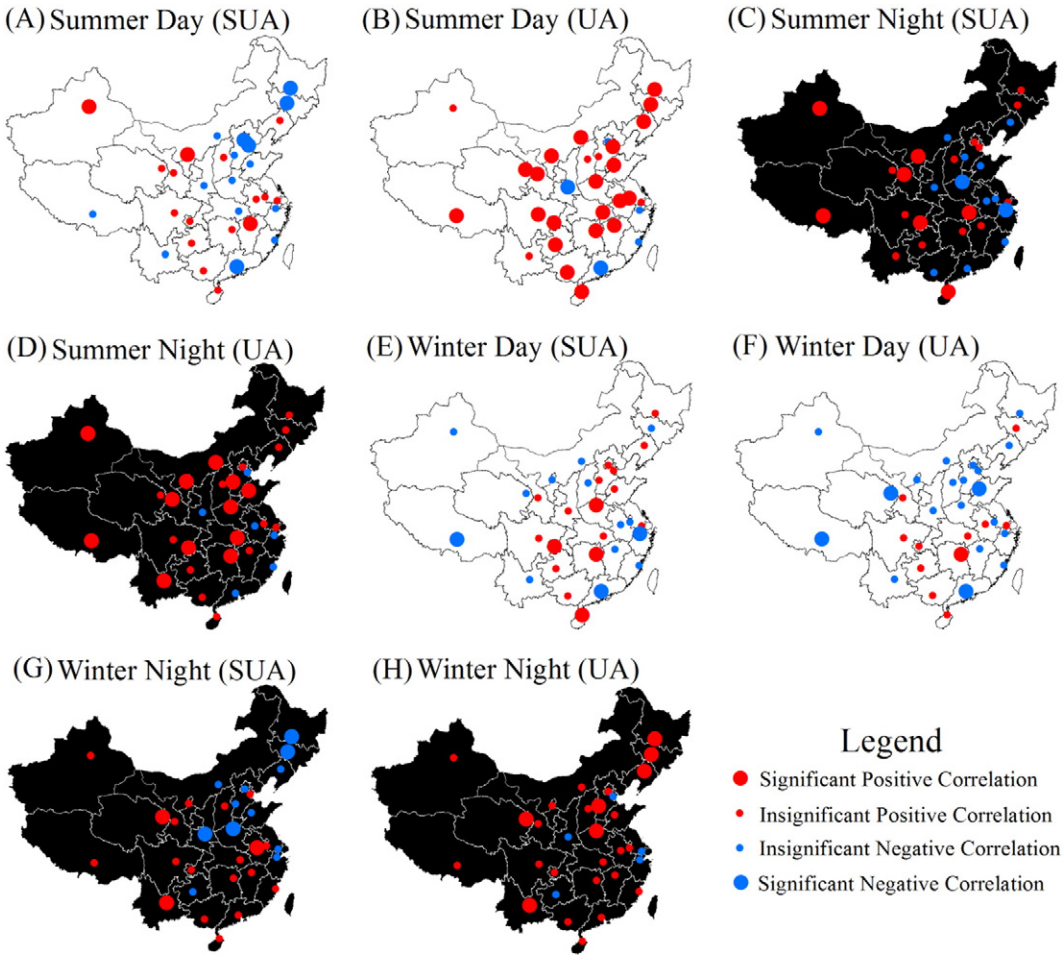

Fig. 10. Pearson's correlation analyses between SUHII and △NL in each city during 2001–2015.

across different cities and results showed the daytime SUHII was significantly positively correlated with air temperature. Zhou et al. (2016a) showed that the inter-annual variability of SUHII was dominated by human activity (urbanization) rather than background climate variability (air temperature and precipitation), however, SUHII was also affected by background climate variability in areas that did not present changes in land cover (SUAs) in this study. High temperatures are usually accompanied by low precipitation, which can lead to low soil moisture, prohibiting evapotranspiration and vegetation growth in rural areas and decreasing the UHI (Piao, 2003; Chuai et al., 2013). Correlation analyses indicated that in most cities, the T_{rural} was negatively and positively correlated with EVI (rural areas) and △EVI, and significant correlations were also observed in several northern cities (Table S2). Piao (2003) and Chuai et al. (2013) showed that NDVI was negatively correlated with air temperature in Northern China in summer. Winguth and Kelp (2013) also showed that in Dallas (US), drought and heat wave events caused an urban cold island (−2.3 °C) in July 2011 at 11:00 am, which was close to the local solar time (10:30 am) of Terra satellite data used in this study. In addition, studies have shown that the UHI can be amplified by heat waves (Li and Bou-Zeid, 2013; Ramamurthy and Bou-Zeid, 2017), however, UHI was compared for different dates in the same year in these studies and the vegetation activity will not change greatly within a few days. Spatially, the number of cities with significant correlations between SUHII and T_{rural} in northern China (8 out of 15) were much greater than the corresponding number in southern China (2 out of 15). Northern China is mainly characterized by arid, semi-arid and semi-humid climate, the soil moisture in northern cities were lower than those in southern cities (humid climate), so northern cities are more sensitive to high air temperature and low precipitation (Buyantuyev and Wu, 2012). Although the reasons for negative correlations between SUHII and T_{rural} in winter days for most cities (especially in northern China) remains unclear, lower temperature may lead to higher energy consumption (e.g., coal burned for heating) in urban areas and then increase the SUHII, especially in northern China (Zhou et al., 2014).

In this study, the SUHII in UAs was positively correlated with △NL in most cities in summer days, summer nights and winter nights. The number of cities with significant positive correlations between SUHII and △NL in UAs was 21, 12 and 7 in summer days, summer nights and winter nights, respectively, which suggests that the increasing △NL was an important factor correlating with SUHII in UAs. The rate of urbanization was much faster in UAs than in rural areas, which led to a more rapid increasing anthropogenic heat release and increases in SUHII for UAs. These results are similar to previous studies (Peng et al., 2012; Zhou et al., 2014).

In summary, the reduction of vegetation coverage and increasing anthropogenic heat release led to increases in SUHII in areas that have experienced land cover change (UAs). However, the SUHII during daytime in SUAs was affected by background climate variability (rural LST).

Several uncertainties affect the results presented in this study. First, the negative correlations between SUHII in SUAs and T_{rural} for most cities in winter days were not clear. Thus, additional experiments and ground observations should be conducted in future. Second, a greater number of UHI-related factors should be considered in the correlation analyses, especially albedo information, the most important factor for the nighttime SUHII (Peng et al., 2012; Zhou et al., 2014). We did not use the MODIS albedo because these data contain a considerable number of gaps. Third, the number of cities with significant correlations

between SUHII and associated determinants was generally less than half of those surveyed except in summer days in UAs. In addition, the 15-year period may be too short to reveal significant trends, thus, longer period work should be included in future studies.

5. Conclusion

In this study, MODIS LST data and CLUDs were used to investigate the temporal trends of SUHI in 31 major cities in China for the period 2001–2015. Correlation analyses were conducted between SUHII and background LST, vegetation coverage and anthropogenic heat release in each city across the years studied. The SUHI averaged from 2001 to 2015 was characterized by large spatiotemporal heterogeneity, and the highest SUHII and largest $Area_{SUHI}$ and $Area_{SSUHI}$ were observed in summer days, whereas the lowest SUHII and smallest $Area_{SUHI}$ and $Area_{SSUHI}$ were observed in winter days. The SUHII was higher in southern China than northern China in summer days and winter days, whereas the opposite occurred in summer nights and winter nights.

Inter-annually, the SUHII in UAs and $Area_{SUHI}$ and $Area_{SSUHI}$ in most cities increased significantly in summer days. In summer nights and winter nights, the SUHII increased significantly in nearly half of the cities, and significant increasing trends of $Area_{SUHI}$ and $Area_{SSUHI}$ were observed in more than half of the cities. The increasing rates of nighttime SUHII in northern cities were nearly twice as high as those in southern cities. In winter days, increasing trends of SUHI were observed in southern cities, whereas the opposite results were observed in northern cities. In summer days, summer nights and winter nights, the SUHII increased in approximately 80% and >50% of the area in union areas and 20 km buffer zones, respectively.

The correlation analyses showed that the SUHII in SUAs was negatively correlated with background LSTs in most cities in summer days and winter days, especially in northern China. The decreasing vegetation coverage contributed to the increasing SUHII in summer days and the rising SUHII in summer nights in UAs. Interestingly, the SUHII was significant negatively correlated with △EVI in several southern cities but significant positively correlated with △EVI in certain northern cities in winter. The increasing anthropogenic heat release was also an important reason for the increasing SUHII in UAs.

In summary, the SUHIs are intensifying in China, measures for mitigating SUHIs should be taken to prevent the deterioration of our living environment.

Appendix A. Supplementary data

Supplementary data to this article can be found online at http://dx.doi.org/10.1016/j.scitotenv.2017.07.217.

References

Akbari, H., Cartalis, C., Kolokotsa, D., Muscio, A., Pisello, A.L., Rossi, F., Santamouris, M., Synnefa, A., Wong, N.H., Zinzi, M., 2015. Local climate change and urban heat island mitigation techniques – the state of the art. J. Civ. Eng. Manag. 22, 1–16.

Arnfield, A.J., 2003. Two decades of urban climate research: a review of turbulence exchanges of energy and water and the urban heat island. Int. J. Climatol. 23, 1–26.

Buyantuyev, A., Wu, J., 2012. Urbanization diversifies land surface phenology in arid environments: interactions among vegetation, climatic variation, and land use pattern in the Phoenix metropolitan region, USA. Landsc. Urban Plan. 105, 149–159.

Chen, T., Huang, Q., Liu, M., Li, M., Qu, L.a., Deng, S., Chen, D., 2017. Decreasing net primary productivity in response to urbanization in Liaoning province, China. Sustain. For. 9, 162.

Chuai, X., Huang, X., Wang, W., Bao, G., 2013. NDVI, temperature and precipitation changes and their relationships with different vegetation types during 1998–2007 in Inner Mongolia, China. Int. J. Climatol. 33, 1696–1706.

Clinton, N., Gong, P., 2013. MODIS detected surface urban heat islands and sinks: global locations and controls. Remote Sens. Environ. 134, 294–304.

Doick, K.J., Peace, A., Hutchings, T.R., 2014. The role of one large greenspace in mitigating London's nocturnal urban heat island. Sci. Total Environ. 493, 662–671.

Du, H., Wang, D., Wang, Y., Zhao, X., Qin, F., Jiang, H., Cai, Y., 2016. Influences of land cover types, meteorological conditions, anthropogenic heat and urban area on surface urban heat island in the Yangtze River Delta Urban Agglomeration. Sci. Total Environ. 571, 461–470.

Elvidge, C.D., Ziskin, D., Baugh, K.E., Tuttle, B.T., Ghosh, T., Pack, D.W., Erwin, E.H., Zhizhin, M., 2009. A fifteen year record of global natural gas flaring derived from satellite data. Energies 2, 595–622.

Grimm, N.B., Faeth, S.H., Golubiewski, N.E., Redman, C.L., Wu, J., Bai, X., et al., 2008. Global change and the ecology of cities. Science 319, 756–760.

Han, G., Xu, J., 2013. Land surface phenology and land surface temperature changes along an urban-rural gradient in Yangtze River Delta, china. Environ. Manag. 52, 234–249.

Huang, X., Schneider, A., Friedl, M.A., 2016. Mapping sub-pixel urban expansion in China using MODIS and DMSP/OLS nighttime lights. Remote Sens. Environ. 175, 92–108.

Imhoff, M.L., Bounoua, L., DeFries, R., Lawrence, W.T., Stutzer, D., Tucker, C.J., Ricketts, T., 2004. The consequences of urban land transformation on net primary productivity in the United States. Remote Sens. Environ. 89, 434–443.

Imhoff, M.L., Zhang, P., Wolfe, R.E., Bounoua, L., 2010. Remote sensing of the urban heat island effect across biomes in the continental USA. Remote Sens. Environ. 114, 504–513.

Kuang, W., Liu, J., Dong, J., Chi, W., Zhang, C., 2016. The rapid and massive urban and industrial land expansions in China between 1990 and 2010: a CLUD-based analysis of their trajectories, patterns, and drivers. Landsc. Urban Plan. 145, 21–33.

Li, D., Bou-Zeid, E., 2013. Synergistic interactions between urban heat islands and heat waves: the impact in cities is larger than the sum of its parts. J. Appl. Meteorol. Climatol. 52, 2051–2064.

Liang, S., Shi, P., Li, H., 2016. Urban spring phenology in the middle temperate zone of China: dynamics and influence factors. Int. J. Biometeorol. 60, 531–544.

Liu, J., Zhang, Z., Xu, X., Kuang, W., Zhou, W., Zhang, S., Li, R., Yan, C., Yu, D., Wu, S., Jiang, N., 2010. Spatial patterns and driving forces of land use change in China during the early 21st century. J. Geogr. Sci. 20, 483–494.

Liu, Z., He, C., Zhang, Q., Huang, Q., Yang, Y., 2012. Extracting the dynamics of urban expansion in China using DMSP-OLS nighttime light data from 1992 to 2008. Landsc. Urban Plan. 106, 62–72.

Liu, J., Kuang, W., Zhang, Z., Xu, X., Qin, Y., Ning, J., Zhou, W., Zhang, S., Li, R., Yan, C., Wu, S., Shi, X., Jiang, N., Yu, D., Pan, X., Chi, W., 2014. Spatiotemporal characteristics, patterns, and causes of land-use changes in China since the late 1980s. J. Geogr. Sci. 24, 195–210.

Maimaitiyiming, M., Ghulam, A., Tiyip, T., Pla, F., Latorre-Carmona, P., Halik, Ü., Sawut, M., Caetano, M., 2014. Effects of green space spatial pattern on land surface temperature: implications for sustainable urban planning and climate change adaptation. ISPRS J. Photogramm. Remote Sens. 89, 59–66.

Pan, J., 2015. Area delineation and spatial-temporal dynamics of urban heat island in Lanzhou city, China using remote sensing imagery. J. Indian Soc. Remote Sens. 44, 111–127.

Peng, S., Piao, S., Ciais, P., Friedlingstein, P., Ottle, C., Breon, F.M., Nan, H., Zhou, L., Myneni, R.B., 2012. Surface urban heat island across 419 global big cities. Environ. Sci. Technol. 46, 696–703.

Piao, S., 2003. Interannual variations of monthly and seasonal normalized difference vegetation index (NDVI) in China from 1982 to 1999. J. Geophys. Res. 108.

Qiao, Z., Tian, G., Xiao, L., 2013. Diurnal and seasonal impacts of urbanization on the urban thermal environment: a case study of Beijing using MODIS data. ISPRS J. Photogramm. Remote Sens. 85, 93–101.

Qiao, Z., Tian, G., Zhang, L., Xu, X., 2014. Influences of urban expansion on urban heat island in Beijing during 1989–2010. Adv. Meteorol. 2014, 1–11.

Quan, J., Zhan, W., Chen, Y., Wang, M., Wang, J., 2016. Time series decomposition of remotely sensed land surface temperature and investigation of trends and seasonal variations in surface urban heat islands. J. Geophys. Res. Atmos. 121, 2638–2657.

Ramamurthy, P., Bou-Zeid, E., 2017. Heatwaves and urban heat islands: a comparative analysis of multiple cities. J. Geophys. Res. Atmos. 122, 168–178.

Roman, K.K., O'Brien, T., Alvey, J.B., Woo, O., 2016. Simulating the effects of cool roof and PCM (phase change materials) based roof to mitigate UHI (urban heat island) in prominent US cities. Energy 96, 103–117.

Shen, H., Huang, L., Zhang, L., Wu, P., Zeng, C., 2016. Long-term and fine-scale satellite monitoring of the urban heat island effect by the fusion of multi-temporal and multi-sensor remote sensed data: a 26-year case study of the city of Wuhan in China. Remote Sens. Environ. 172, 109–125.

Song, K., Wang, M., Du, J., Yuan, Y., Ma, J., Wang, M., Mu, G., 2016. Spatiotemporal variations of lake surface temperature across the Tibetan plateau using MODIS LST product. Remote Sens. 8, 854.

Tao, J., Zhang, L., Cao, J., Zhong, L., Chen, D., Yang, Y., Chen, D., Chen, L., Zhang, Z., Wu, Y., Xia, Y., Ye, S., Zhang, R., 2017. Source apportionment of $PM_{2.5}$ at urban and suburban areas of the Pearl River Delta region, south China - with emphasis on ship emissions. Sci. Total Environ. 574, 1559–1570.

Tiangco, M., Lagmay, A.M.F., Argete, J., 2008. ASTER-based study of the night-time urban heat island effect in metro manila. Int. J. Remote Sens. 29, 2799–2818.

Tran, H., Uchihama, D., Ochi, S., Yasuoka, Y., 2006. Assessment with satellite data of the urban heat island effects in Asian mega cities. Int. J. Appl. Earth Obs. Geoinf. 8, 34–48.

Tu, L., Qin, Z., Li, W., Geng, J., Yang, L., Zhao, S., Zhan, W., Wang, F., 2016. Surface urban heat island effect and its relationship with urban expansion in Nanjing, China. J. Appl. Remote. Sens. 10, 026037.

United Nations, 2014. World Urbanization Prospects: The 2013 Revision.

Wan, Z., 2008. New refinements and validation of the MODIS land-surface temperature/emissivity products. Remote Sens. Environ. 112, 59–74.

Wang, F., Ge, Q., Wang, S., Li, Q., Jones, P.D., 2015a. A new estimation of urbanization's contribution to the warming trend in China. J. Clim. 28, 8923–8938.

Wang, J., Huang, B., Fu, D., Atkinson, P., 2015b. Spatiotemporal variation in surface urban heat island intensity and associated determinants across major Chinese cities. Remote Sens. 7, 3670–3689.

Wang, Y., Berardi, U., Akbari, H., 2016a. Comparing the effects of urban heat island mitigation strategies for Toronto, Canada. Energ. Buildings 114, 2–19.

Wang, C., Myint, S., Wang, Z., Song, J., 2016b. Spatio-temporal modeling of the urban heat island in the Phoenix metropolitan area: land use change implications. Remote Sens. 8, 185.
Ward, K., Lauf, S., Kleinschmit, B., Endlicher, W., 2016. Heat waves and urban heat islands in Europe: a review of relevant drivers. Sci. Total Environ. 569-570, 527–539.
Weng, Q., 2002. Land use change analysis in the Zhujiang Delta of China using satellite remote sensing, GIS and stochastic modelling. J. Environ. Manag. 64, 273–284.
Weng, Q., Liu, H., Liang, B., Lu, D., 2008. The spatial variations of urban land surface temperatures: pertinent factors, zoning effect, and seasonal variability. IEEE J-STARS 1 (2), 154–166.
Weng, Q., Fu, P., Gao, F., 2014. Generating daily land surface temperature at Landsat resolution by fusing Landsat and MODIS data. Remote Sens. Environ. 145, 55–67.
Winguth, A.M.E., Kelp, B., 2013. The urban heat island of the north-central Texas region and its relation to the 2011 severe Texas drought. J. Appl. Meteorol. Climatol. 52, 2418–2433.
Yao, R., Wang, L., Huang, X., Guo, X., Niu, Z., Liu, H., 2017. Investigation of urbanization effects on land surface phenology in northeast china during 2001–2015. Remote Sens. 9 (*1*):66. http://dx.doi.org/10.3390/rs9010066.
Zhang, J., Wang, Y., 2008. Study of the relationships between the spatial extent of surface urban heat islands and urban characteristic factors based on Landsat ETM + data. Remote Sens. 8, 7453–7468.
Zhang, L., Weng, Q., 2016. Annual dynamics of impervious surface in the Pearl River Delta, China, from 1988 to 2013, using time series Landsat imagery. ISPRS J. Photogramm. Remote Sens. 113, 86–96.
Zhang, X., Friedl, M.A., Schaaf, C.B., Strahler, A.H., Schneider, A., 2004. The footprint of urban climates on vegetation phenology. Geophys. Res. Lett. 31, L12209.
Zhao, M., Cai, H., Qiao, Z., Xu, X., 2016. Influence of urban expansion on the urban heat island effect in Shanghai. Int. J. Geogr. Inf. Sci. 30, 2421–2441.
Zhou, D., Zhao, S., Liu, S., Zhang, L., Zhu, C., 2014. Surface urban heat island in China's 32 major cities: spatial patterns and drivers. Remote Sens. Environ. 152, 51–61.
Zhou, D., Zhao, S., Zhang, L., Sun, G., Liu, Y., 2015. The footprint of urban heat island effect in China. Sci Rep 5, 11160.
Zhou, D., Zhang, L., Hao, L., Sun, G., Liu, Y., Zhu, C., 2016a. Spatiotemporal trends of urban heat island effect along the urban development intensity gradient in China. Sci. Total Environ. 544, 617–626.
Zhou, D., Zhang, L., Li, D., Huang, D., Zhu, C., 2016b. Climate–vegetation control on the diurnal and seasonal variations of surface urban heat islands in China. Environ. Res. Lett. 11, 074009.
Zhou, D., Zhao, S., Zhang, L., Liu, S., 2016c. Remotely sensed assessment of urbanization effects on vegetation phenology in China's 32 major cities. Remote Sens. Environ. 176, 272–281.